

# An open-source 3D Slicer module for fluoro-free transcatheter vessel navigation

Hareem Nisar<sup>a,b</sup>, Patrick Carnahan<sup>a,b</sup>, Daniel Bainbridge<sup>c</sup>, Elvis C. S. Chen<sup>a,b,d</sup>, and Terry M. Peters<sup>a,b</sup>

<sup>a</sup>Robarts Research Institute, Canada

<sup>b</sup>School of Biomedical Engineering, Western University, Canada

<sup>c</sup>London Health Sciences Centre, London, Canada

<sup>d</sup>Lawson Health Research Institute, London, Canada

## ABSTRACT

Vascular navigation is an essential component of transcatheter cardiovascular interventions, conventionally performed using either 2D fluoroscopic imaging or CT- derived vascular roadmaps which can lead to many complications for the patients as well as the clinicians. This study presents an open-source and user-friendly 3D Slicer module that performs vessel reconstruction from tracked intracardiac ultrasound (ICE) imaging using deep learning-based methods. We also validate the methods by performing a vessel-phantom study. The results indicate that our Slicer module is able to reconstruct vessels with sufficient accuracy with an average distance error of 0.86 mm. Future work involves improving the speed of the methods as well as testing the module in an in-vivo setting. Clinical adaptation of this platform will allow the clinicians to navigate the vessels in 3D and will potentially enhance their spatial awareness as well as improve procedural safety.

**Keywords:** transcatheter vessel navigation; tracked intracardiac ultrasound (ICE); fluoro-free

## 1. INTRODUCTION

Transcatheter interventions are characterized by their minimally invasive nature, enhanced patient safety, and shorter hospital stays,<sup>1,2</sup> however, they face the challenge of missing a direct line of sight with the tools and the anatomy. Ultrasound, CT, and fluoroscopic imaging are often used in combination to provide sufficient visualization during cardiovascular procedures. Cardiac interventions employ a transfemoral navigation approach where the heart chambers are accessed through a puncture in the femoral artery or the vein and traversing the vessels under fluoroscopic guidance. For endovascular procedures, many vessel branches must be traversed in order to gain access to the target vessel using a CT-derived pre-mapped vascular roadmap or using live X-ray imaging with contrast agents. These current standard-of-care procedures expose the patients as well as the medical staff to harmful radiation causing high-grade skin injury and renal failure in patients and eye cataracts,<sup>3</sup> increased risk of cancer,<sup>4</sup> and thyroid gland disease<sup>5</sup> in the medical team. The lead aprons used to shield the operators are also known to cause back, neck, and spinal issues for interventionalists.<sup>6,7</sup> As an alternative to these radiation-based methods, Nisar et al.<sup>8</sup> proposed an ultrasound-based workflow where a tracked, radial intracardiac echocardiographic (ICE) probe can traverse and scan the vessels and generate a vascular roadmap in 3D for a tracked guidewire to follow. The same group also developed deep learning-based methods for segmenting vessel lumen from ICE imaging in real-time.<sup>9</sup>

In this work, we aim to combine the abovementioned ICE-based vessel navigation workflow with the deep learning-based segmentation methods in order to create a complete, open-source, and user-friendly 3D Slicer module<sup>10</sup> as a prototype of a platform that can be easily used by a clinician. The development of a customized 3D Slicer module allows for the methods to be seamlessly used during in-vivo experiments as well as further testing for clinical usage and feasibility – which is currently a major barrier to the clinical adaptation and widespread use of image-guided systems (IGSs) .<sup>11</sup> In this paper, we present the design of a customized 3D Slicer module which can be used to generate a vascular roadmap for cardiovascular interventions, as well as validating it using a vessel phantom. The accuracy of the ICE-generated vessel is established by comparing it to the CT-derived vascular roadmap.

---

Send correspondence to H.N.: hnisar3@uwo.ca or E.C.S.C : chene@robarts.ca

## 2. METHODS

### 2.1 3D Slicer Module Workflow

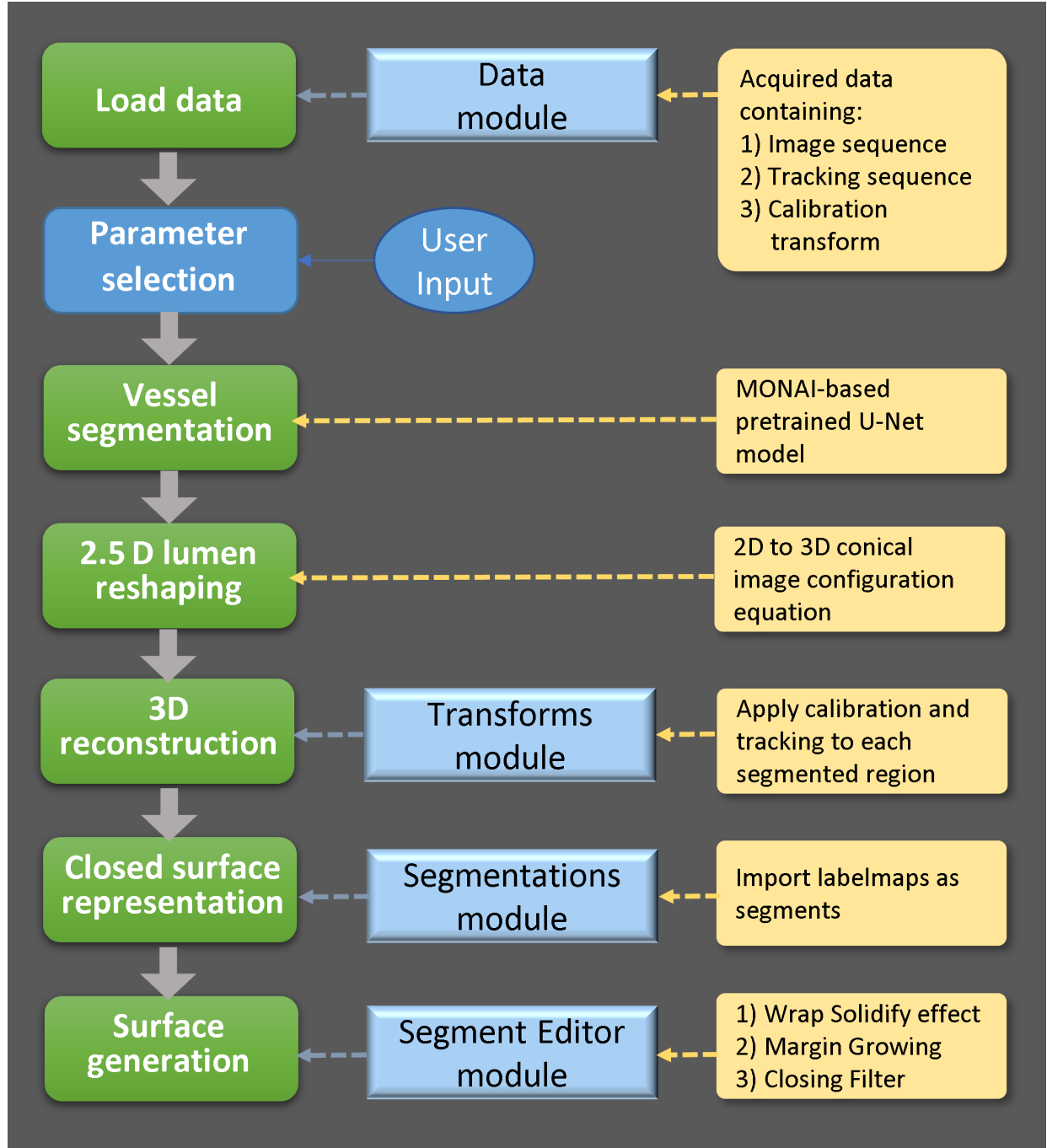


Figure 1. Components of our customized Slicer modules and their dependency on existing Slicer methods.

The Slicer module implements the methods from<sup>8,9</sup> with two major modifications – A) the vessel segmentation portion of the vessel reconstruction pipeline is replaced with a deep learning-based solution provided by,<sup>9</sup> and B) updated methods are used during the last surface reconstruction step. Figure 1 provides an overview of the workflow of the module, as well as indicating existing Slicer modules we utilize in our vascular reconstruction

procedure. The complete Slicer module along with some test data can be found at <https://github.com/hareem-nisar/Vascular-Navigation>. The module framework begins with loading the data (acquired via set-up described in the next section) and ends with producing a 3D model of the vessel surface. A brief description of each of the steps is given below:

- *Load Data:* The vessel (phantom or patient) is scanned using a magnetically tracked, radial ICE probe, and the imaging and tracking data is loaded to a 3D Slicer using the Data module in the form of a “sequence”. The probe calibration matrix is loaded into Slicer as a “transform”.
- *Parameter Selection:* Once the data are correctly loaded into Slicer, the user selects them in our customized module. Additionally, a user can select how many frames they would like to reconstruct from the sequence and the approximate vessel diameter (in pixels). The last parameter i.e., imaging angle is specific to the forward-looking angle of the conical Foresight™ ICE imaging probe.
- *Vessel Segmentation:* The vessel reconstruction algorithm works by first segmenting the vessel lumen region from ICE ultrasound imaging, and then placing the segments in their respective 3D space. In our Slicer implementation, vessel segmentation is performed using deep learning-based methods which allow for real-time processing of imaging frames. A pre-trained U-Net model as described by Nisar et al.<sup>9</sup> processes 2D ICE images and produce a corresponding 2D lumen segment. The model is currently trained on animal (swine) inferior vena cava images acquired using a Foresight™ ICE probe, which is characterized by its 2.5D conical surface images.
- *Lumen Reshaping:* Since the segmented regions are extracted from the 2D, flattened version of a conical, 3D ICE image, an additional step is required to convert the segmentations to their true conical shape. Each segmented region undergoes a reshaping function governed by equation 1, where  $\phi$  denotes the imaging angle of the Foresight™ ICE probe used during data acquisition.

$$\begin{bmatrix} x_{3D} \\ y_{3D} \\ z_{3D} \end{bmatrix} = \begin{bmatrix} 1 & 0 & -o_x \\ 0 & 1 & -o_y \\ 0 & 0 & \|(x_{2D}, y_{2D})\| \tan(90 - \phi) \end{bmatrix} \begin{bmatrix} x_{2D} \\ y_{2D} \\ 1 \end{bmatrix} \quad (1)$$

- *3D Reconstruction:* Next, each segment is operated upon by a calibration matrix using the “Transforms” module, as well as a probe-tracking transform that represents the 3D location of the probe when the respective image was acquired.
- *Closed Surface Representation:* To initiate the surface reconstruction process, a closed surface is created for all of the segmentations, and appended to a polydata structure whose final representation containing the full structure of the desired vessel is then imported as a single segment using the “Segmentations” module.
- *Surface Generation:* Finally, the surface is reconstructed by applying three operations or “effects” from the “Segment Editor” module including wrap solidify effect, followed by margin growing by 1 mm and morphological closing using a 3 mm kernel.

## 2.2 Navigation System and Clinical Workflow

The Slicer module is designed for clinical usage and in-vivo testing and it incorporates a simplified, user-friendly interface to be used by the clinician. Figure 2 shows the schematic layout of a clinical setting where a tabletop magnetic tracking system (MTS) such as the NDI Aurora<sup>12</sup> tabletop tracker is placed on the patient bed to achieve real-time intraoperative tracking of the tools and the ICE probe. The ICE image and tracking data are communicated to 3D Slicer via the PLUS server application<sup>13</sup> and the “OpenIGTLinkIF” module. A single video monitor is required for visualizing the intraoperative motion of tools, ultrasound imaging, and reconstructed vessel in 3D.

In preparation for tracking the ultrasound image, the Foresight™ ICE probe was augmented with a 6DoF magnetic tracking sensor and calibrated using a point-to-line registration method.<sup>14,15</sup> To generate a vascular

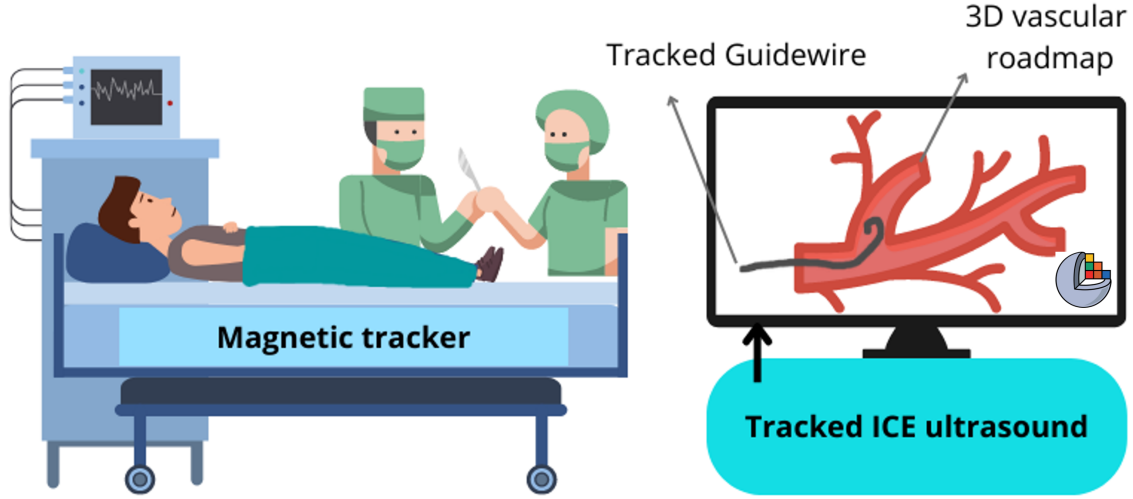


Figure 2. Schematic layout during clinical usage of a vessel navigation platform.

roadmap, the user scans the desired vessels using the tracked ICE probe with the resulting images being processed by the Slicer module to reconstruct a 3D vessel. The user may then introduce a tracked guidewire<sup>16</sup> and follow the vascular roadmap to reach the target organ.

### 2.3 Phantom Validation

The customized module was tested using a phantom experiment. An ultrasound imaging-realistic vessel phantom was placed in the field of a magnetic tracking system (MTS) and scanned using a tracked and calibrated Foresight<sup>TM</sup>ICE probe. The image and tracking data were acquired in the form of a sequence and processed to reconstruct the vessel in 3D. The accuracy of this US-reconstructed vessel is validated by comparing it to the 3D vessel derived from the CT scan of the same phantom.

To compare the US-reconstructed and CT-derived vessel structures, the CT scan was first registered to the tracker coordinates using the divots on the phantom, which were localized in MTS coordinate system using a round-tip pre-tracked stylus that was calibrated using the “Pivot Calibration” module. The divots were also manually identified in the 3D CT imaging volume by placing fiducials using the “Markups” module. The MTS fiducials, after being transformed by the matrix derived from the pivot calibration, were registered to the CT-derived fiducials using the “Fiducial Registration” module. These steps were not incorporated into our Slicer module, as they are only part of our study and not expected in a clinical workflow. After the registration, the common regions between US-reconstructed and CT-derived vessels were compared using the “Segment Comparison” module to determine spatial overlap metrics such as DICE score, specificity, and sensitivity, as well as surface distance error in terms of Hausdorff distance (HD).

## 3. RESULTS

### 3.1 Slicer Module Design

Our Slicer module, designed to reconstruct a vessel from tracked ICE imaging, has three selection buttons as well as three user-controlled parameters in the interface. The module is user-friendly, allowing the user or the clinicians to run all the reconstruction steps with a click of a button. Figure 3 shows the layout for the slicer module that the user will interact with.

The core intermediate stages for 3D vessel reconstruction include: vessel segmentation (figure 4b), 3D placement of segments (figure 4c), and surface reconstruction (figure 4d). These intermediate steps are not clinically relevant and are therefore not presented to the clinician. Upon running the module, the user only sees the final 3D reconstructed vessel as an output figure 4d).

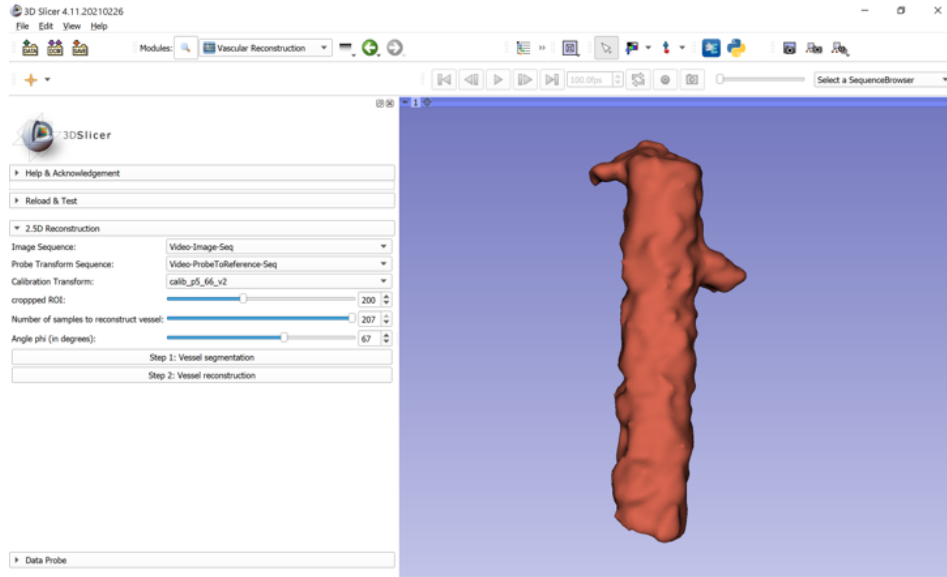


Figure 3. Screenshot of our customized Slicer module showing parameter selection buttons and 3D visualization of the reconstructed vessel.

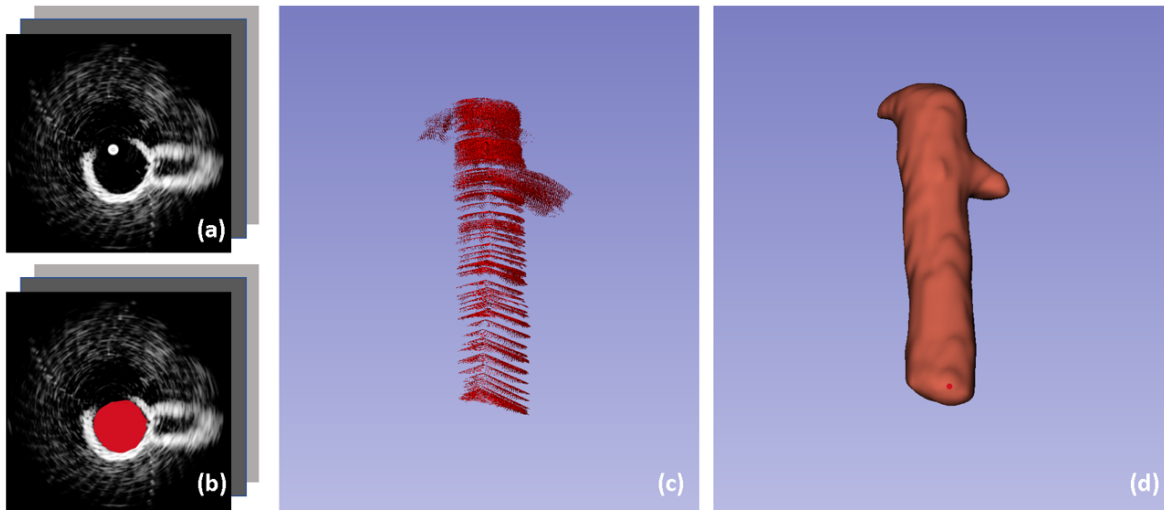


Figure 4. Intermediate processing steps during vessel reconstruction from a sequence of ICE images (a) including vessel lumen segmentation from each frame (b), 3D positioning using tracking and calibration transforms (c), and final output showing 3D surface reconstruction of the vessel (d).

### 3.2 Phantom Experiment Results

The accuracy of the ICE-reconstructed vessel was validated against the vessel segmentation derived from a CT scan of the same phantom. The results indicate that the average Hausdorff distance error between the surfaces is  $0.86 \pm 0.81$  mm with a maximum of 5.04 mm. Figure 5 show a heatmap of the distance error for our ICE-generated vessel with the maximum error regions shown in red. The accuracy of vessel reconstruction in terms of spatial overlap is given in Table 1, where the overall DICE score is 0.86. Only 1.2% of the reconstructed vessel region lied outside the ground truth (false positive). 9.9% of the region was false-negative and was missing from the reconstruction. Overall, the ICE-reconstructed vessel exhibited a lower volume than the ground truth vessel segmentation.

Table 1: Accuracy of the ICE-generated vessel in comparison to the CT-derived vessel

Spatial Overlap	Value	Hausdorff Distance (mm)	Value
Dice coefficient	0.86	Average	0.86
Sensitivity	0.78	95%	2.45
Specificity	0.97	Maximum	5.04

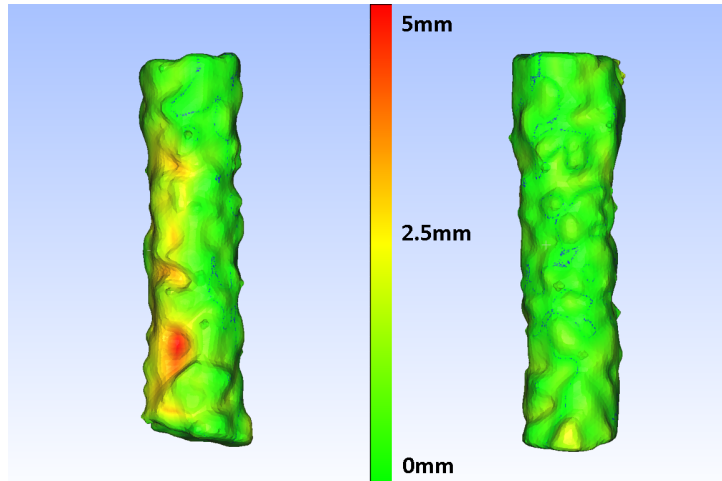


Figure 5. Two different views of the ICE-reconstructed vessel with the colors representing the Hausdorff distance when compared with the CT-derived ground truth.

## 4. DISCUSSION

Vessel navigation is an essential task performed during transcatheter cardiovascular interventions. Currently, transfemoral navigation performed using fluoroscopy which leads to radiation exposure, use of lead shielding, and associated health risks to the patient and the medical team. ICE imaging is often employed during interventions to guide the procedures. Literature includes alternative methods such as a no-fluoro, ICE ultrasound-based reconstruction of a vascular roadmap, as well as real-time vessel segmentation methods compatible with ICE imaging. However, these studies are in their early stage and require further in-vivo testing and experiments, which necessitates a user-friendly interface that can be used by clinicians.

In this study, we present a customized 3D Slicer module that integrates and improvise the methods from<sup>9</sup> and<sup>8</sup> to create a seamless platform that performs vascular reconstruction from the tracked ICE imaging of the desired vessel. We tested the module on a dual-layered vessel phantom,<sup>17</sup> and compared the output vessel with CT-derived ground truth. The results indicate an average surface distance error of  $0.86 \pm 0.81$  mm which,

according to the clinicians with whom we collaborate, is an acceptable range of accuracy for the task of vessel navigation (less than 5 mm).

During navigation of the ICE-generated vascular roadmap, the distal tool-tip is likely to damage or puncture a vessel wall if the boundary of the reconstructed vessel lies outside the real vessel wall. In such a case, the user will have misleading information i.e., the tool tip is within the vessel lumen when in fact it is at or outside the vessel boundary. In terms of spatial overlap, we observe that overall, the ICE-reconstructed vessel lies within the ground truth vessel and only 1.2% of the vessel region falsely lies outside the ground truth indicating a minimal error.

Another important clinical requirement is the speed of the vessel reconstruction which ideally should be near real-time. While the vessel segmentation component of our module is near real-time, the 3D surface reconstruction pipeline is time-consuming and can take several minutes depending on the length of the vessel and parameters chosen by the clinician. There is room for improvement as the current algorithm is implemented sequentially using Python and can be accelerated by employing a lower-level language, as well as considering asynchronous and GPU-based programming.

It should be noted that our current methods are designed for Conavi's Foresight™ ICE imaging system which produces a 2D conical surface image that lies within 3D space, and the vessel reconstruction pipeline includes an additional step of interpolating the 2D segmentations to their 3D conical form which also contributes to the vessel reconstruction time. The module can be trivially modified to accommodate other radial ultrasound probes by eliminating this additional reshaping step while maintaining the remainder of the methods. Doing so will also increase processing speed to some extent.

The accuracy results presented in this paper are representative of a phantom study and may differ for animal or in-vivo vessel reconstruction. The primary reason is that the U-Net-based model employed for vessel segmentation was trained on an animal vessel (inferior vena cava) imaging and not the phantom. Future work can potentially include validating our 3D Slicer module in an in-vivo pig study where the complete inferior vena cava will be scanned using a tracked, radial ICE probe and reconstructed using the module. A tracked guidewire will then follow the vascular roadmap and its position will be confirmed using fluoroscopy.

## 5. CONCLUSION

Vessel reconstruction in 3D has the potential to provide more contextual information to clinicians, and move towards fluoro-free cardiovascular interventions. While methods for real-time vessel segmentation and ultrasound-based vessel reconstruction are part of the literature, further experimentation and in-vivo validation of these methods necessitate a simplified, user-friendly user interface. In this paper, we presented an easy-to-use 3D Slicer module that integrates all the methods required for ICE-based vessel reconstruction and can be intuitively used by a clinician to generate a vascular roadmap for navigation. The results indicate that the customized Slicer module provides sufficient accuracy for vessel reconstruction, as verified by the phantom experiment, and can be used for future in-vivo experiments.

## Acknowledgement

The authors would like to thank Conavi Medical Inc. for their continuous support through this project.

## Funding

We acknowledge our sources of funding from the Canadian Institutes of Health Research (CIHR) (FDN 201409) and Canadian Foundation for Innovation (CFI) (LEF 36199). The grants are held by Dr. Terry Peters.

## REFERENCES

- [1] Arora, S., Strassle, P. D., Kolte, D., Ramm, C. J., Falk, K., Jack, G., Caranasos, T. G., Cavender, M. A., Rossi, J. S., and Vavalle, J. P., “Length of stay and discharge disposition after transcatheter versus surgical aortic valve replacement in the united states,” *Circulation: Cardiovascular Interventions* **11**(9), e006929 (2018).
- [2] Latif, A., Lateef, N., Ahsan, M. J., Kapoor, V., Usman, R. M., Cooper, S., Andukuri, V., Mirza, M., Ashfaq, M. Z., and Khouzam, R., “Transcatheter Versus Surgical Aortic Valve Replacement in Patients with Cardiac Surgery: Meta-Analysis and Systematic Review of the Literature,” *Journal of Cardiovascular Development and Disease* **7**, 36 (Sep 2020).
- [3] Jacob, S., Boveda, S., Bar, O., Brézin, A., Maccia, C., Laurier, D., and Bernier, M. O., “Interventional cardiologists and risk of radiation-induced cataract: Results of a French multicenter observational study,” *International Journal of Cardiology* **167**, 1843–1847 (Sep 2013).
- [4] Roguin, A., Goldstein, J., Bar, O., and Goldstein, J. A., “Brain and neck tumors among physicians performing interventional procedures,” *American Journal of Cardiology* **111**, 1368–1372 (May 2013).
- [5] Volzke, H., Werner, A., Wallaschofski, H., Friedrich, N., Robinson, D. M., Kindler, S., Kraft, M., John, U., and Hoffmann, W., “Occupational exposure to ionizing radiation is associated with autoimmune thyroid disease,” *Journal of Clinical Endocrinology and Metabolism* **90**, 4587–4592 (Aug 2005).
- [6] Ross, A. M., Segal, J., Borenstein, D., Jenkins, E., and Cho, S., “Prevalence of Spinal Disc Disease Among Interventional Cardiologists,” *The American Journal of Cardiology* **79**, 68–70 (Jan 1997).
- [7] Klein, L. W., Tra, Y., Garratt, K. N., Powell, W., Lopez-Cruz, G., Chambers, C., and Goldstein, J. A., “Occupational health hazards of interventional cardiologists in the current decade: Results of the 2014 SCAI membership survey,” *Catheterization and Cardiovascular Interventions* **86**, 913–924 (Nov 2015).
- [8] Nisar, H., Groves, L., Cardarelli-Leite, L., Peters, T. M., and Chen, E. C., “Toward Fluoro-Free Interventions: Using Radial Intracardiac Ultrasound for Vascular Navigation,” *Ultrasound in Medicine and Biology* **48**, 1290–1298 (Jul 2022).
- [9] Nisar, H., Fakim, D., Bainbridge, D., Chen, E. C. S., and Peters, T., “3D localization of vena contracta using Doppler ICE imaging in tricuspid valve interventions,” *International Journal of Computer Assisted Radiology and Surgery* , 1–9 (May 2022).
- [10] Fedorov, A., Beichel, R., Kalpathy-Cramer, J., Finet, J., Fillion-Robin, J.-C., Pujol, S., Bauer, C., Jennings, D., Fennessy, F., Sonka, M., Buatti, J., Aylward, S., Miller, J. V., Pieper, S., and Kikinis, R., “3D Slicer as an image computing platform for the Quantitative Imaging Network,” *Magnetic resonance imaging* **30**, 1323–41 (Nov 2012).
- [11] DiMaio, S., Kapur, T., Cleary, K., Aylward, S., Kazanzides, P., Vosburgh, K., Ellis, R., Duncan, J., Farahani, K., Lemke, H., Peters, T., Lorensen, W. B., Gobbi, D., Haller, J., Clarke, L. L., Pizer, S., Taylor, R., Galloway, R., Fichtinger, G., Hata, N., Lawson, K., Tempny, C., Kikinis, R., and Jolesz, F., “Challenges in image-guided therapy system design,” *NeuroImage* **37**(SUPPL. 1), S144–S151 (2007).
- [12] “NDI Aurora - Medical,” (2022). <https://www.ndigital.com/medical/products/aurora/>.
- [13] Lasso, A., Heffter, T., Rankin, A., Pinter, C., Ungi, T., and Fichtinger, G., “PLUS: Open-Source Toolkit for Ultrasound-Guided Intervention Systems,” *IEEE Transactions on Biomedical Engineering* **61**, 2527–2537 (Oct 2014).
- [14] Nisar, H., Moore, J., Alves, N., Hwang, G., Peters, T. M., and Chen, E. C. S., “Ultrasound calibration for unique 2.5D conical images,” in [*SPIE Medical Imaging 2019: Image-Guided Procedures, Robotic Interventions, and Modeling*], Fei, B. and Linte, C. A., eds., **10951**, 573 – 582, International Society for Optics and Photonics (2019).
- [15] Chen, E. C. S., McLeod, A. J., Baxter, J. S. H., and Peters, T. M., “Registration of 3D shapes under anisotropic scaling,” *International Journal of Computer Assisted Radiology and Surgery* **10**, 867–878 (Jun 2015).
- [16] Piazza, R., Nisar, H., Moore, J., Condino, S., Ferrari, M., Ferrari, V., Peters, T. M., and Chen, E. C. S., “Towards electromagnetic tracking of J-tip guidewire: precision assessment of sensors during bending tests,” in [*SPIE Medical Imaging 2020: Image-Guided Procedures, Robotic Interventions, and Modeling*], Fei, B. and Linte, C. A., eds., **11315**, 37–46, International Society for Optics and Photonics (2020).



- [17] Nisar, H., Moore, J., Piazza, R., Maneas, E., Chen, E. C., and Peters, T. M., “A simple, realistic walled phantom for intravascular and intracardiac applications,” *International Journal of Computer Assisted Radiology and Surgery* **15**, 1513–1523 (Sep 2020).